NUMERICAL INVESTIGATIONS IN THREE-DIMENSIONAL INTERNAL FLOWS

SEMI-ANNUAL STATUS REPORT

1 JANUARY THROUGH 30 JUNE 1993

Prepared for:

NASA-AMES RESEARCH CENTER

MOFFETT FIELD, CA 94035

UNDER NASA GRANT

NCC 2-507

By:

WILLIAM C. ROSE

ENGINEERING RESEARCH AND DEVELOPMENT CENTER

UNIVERSITY OF NEVADA, RENO
RENO, NV 89557

I. BACKGROUND

NASA has an ongoing interest in supersonic and hypersonic inlet flowfield research. Their research efforts are intended to complement prospective aerospace vehicles, such as the High-Speed Civilian Transport (HSCT) and the National Aerospace Plane (NASP), as well as other variants of these vehicles intended for use with air-breathing propulsion systems. Computational Fluid Dynamics (CFD) is expected to play a large part in the design and analysis of such aircraft because experimental facilities are limited. The purpose of this Grant is to apply, evaluate and validate CFD tools for use in high-speed inlet flowfields.

In previous efforts under the current Grant, a two-dimensional full Navier-Stokes (FNS) code (SCRAM2D) was used in a design process that involved parametric modifications of the inlet geometry to arrive at what appeared to be an optimum inlet flowfield having a uniform flow at the exit in a very short distance. In these previous studies, the technologies for determining the contours with a "man-in-the-loop" approach for both the ramp and cowl of the inlet were demonstrated and nearly shock-free exiting flowfields were shown to be obtainable. The resulting two-dimensional compression contours were then used with swept sidewalls to form a three-dimensional inlet. Then the three-dimensional Navier-Stokes code (SCRAM3D) was used to investigate the inlet's three-dimensional flow.

Also in previous efforts under the current Grant, 2D and 3D space-marched Navier-Stokes codes were applied to inlet flowfield analysis. It was shown that by using the STUFF code, a space-marched, thin-layer Navier-Stokes code developed and used by Greg Molvik of the MCAT Institute at NASA-Ames, considerable time reductions could be obtained by solving the flowfield that behaves parabolically and then matching the output

of that code to the input of an FNS code such as SCRAM2D or SCRAM3D (or the time-marched version of STUFF called TUFF). In a previous status report, the validity of this process and the accuracy of using the STUFF code were demonstrated by direct comparison with experimental data obtained from the NASA-Lewis Mach 5 inlet study.

Most efforts conducted under this Grant have examined the flowfield characteristics and performance of isolated inlet systems. In reality, of course, these inlet systems are installed on aircraft at various locations. The primary effect on the inlet of installation on an aircraft is the modification of the incoming flowfield and, particularly, an increase in the boundary layer thickness relative to the cowl height. In the previous progress report, the hybrid method of using the STUFF and SCRAM2D codes was applied to the Lewis/Langley Mach 5 waverider aircraft and the impact of the forebody flow (considered in a 2D sense) on the inlet was determined.

II. INTRODUCTION

In the present reporting period, the 3D STUFF code was used to solve the underbody flow for the vehicle shown in Figure 1. In order to start the space-marched version of the code, the time-marched version (TUFF) was used to solve the forward portion of the underside of the forebody flowfield. A grid was generated which went from the tip of the nose to the location of the cowl lip. This includes all of the inlet ramp system. Previous indications were that three-dimensional effects could be expected on the ramps of such an aircraft. For purposes of the present study, no sidewalls were assumed. The sidewalls were eliminated to simplify the calculations and to show the potential effects of three-dimensional flow in the absence of a full sidewall. Further, this flow was also analyzed using the newly released OVERFLOW code and comparisons between the two codes were made. In addition to these 3D calculations, 2D calculations using the OVERFLOW code were also obtained for the Mach 5 inlet model in this reporting period. Comparisons between the experimental data, previous CFD results and those from OVERFLOW were made.

III. RESULTS AND DISCUSSION

The flow was solved on the underside of the geometry depicted in Figure 1 using the TUFF and STUFF codes. The TUFF code was used near the nose, while the STUFF code was used for the rest of the forebody solution. Mach number contours and particle traces near the surface of the inlet ramps are shown in Figure 2. Figure 2 shows the development of the boundary layer along the body up to the origin of the inlet ramps. Downstream of this origin, particle traces are shown that indicate a lateral spillage effect from the outboard module ahead of the cowl lip. A more detailed picture of these particle traces is shown in Figure 3. Figure 3 indicates that the flow in the inboard module remains essentially two-dimensional, while large flow angularity near the surface is seen for the outboard module.

The three-dimensional flowfield characterized by the behavior discussed in Figures 2 and 3 results from the pressure field on the ramp surfaces of the outboard module in the absence of the full sidewall, as shown in Figure 4. Figure 4 shows a prominent expansion around the inlet/airframe corner that leads to the large lateral flow components. The three-dimensional pressure field at the cowl lip station can be characterized clearly through the pressure contours shown in Figure 5. Figure 5 clearly indicates the expansion occurring in the crossflow plane containing the cowl lip. The Mach number contours in this same crossflow plane are depicted in Figure 6 and indicate the same type of behavior.

The lack of an outboard sidewall has a dramatic effect on any subsequent internal flow, as shown clearly in Figure 7. Figure 7 shows the Mach number contours in streamwise planes on the inlet ramps on the centerplane of the vehicle, on the centerplane of the outboard module and near the outer edge of the outboard module. The former two indicate a relatively two-dimensional flowfield, while the Mach number contours located

near the outboard edge of the outboard module indicate a poorly-formed shock wave system that will have an adverse effect on any inlet placed at the back of this ramp system. This adverse effect can be quantified with the aid of the following figures.

Figure 8 shows the streamwise location of two rake positions singled out for discussion here. The Mach number contours and radial position of the rakes to be discussed are shown in Figure 9. These figures show the locations of the rakes along which the Mach number profiles will be shown. Figure 10 shows the Mach number profiles obtained from the 3D solution just ahead of the 4.1 degree ramp at the three positions indicated in Figure 9a. It is clear that the boundary layer thickness is reduced near the outboard edge, as indicated qualitatively in the previous figures. Figure 11 shows the Mach number contours obtained for the four rake locations indicated in Figure 9b and, in addition, indicates the height of the cowl relative to the calculated Mach number profiles. It is clear from this study that near the centerplane and for the inboard module, a "shock on cowl lip" flow is obtained. However, for the mid-outboard module and near the outer edge of the outboard module, the ramp shocks fall inside the cowl lip and flow at the freestream Mach number will be ingested into the inlet. This is due to the previously discussed, ill-formed shock structure associated with the pressure relief around the outboard edge of the ramp system. The ingestion of virtually uncompressed freestream flow into the inlet will result in severely reduced inlet (thus, propulsion) performance. The conclusion from this portion of the study is that sidewalls of some sort must be added to this vehicle to prevent this behavior.

Although large reductions in computational time were obtained by using the STUFF and TUFF codes over that used by the SCRAM3D code for solving the forebody flowfield, large amounts of time (upwards of 10 hours of Cray C-90 CPU time) were used in

obtaining the combined TUFF and STUFF solutions. Most (about 90%) of this time was used by the TUFF code. In the present reporting period, another newly developed code called OVERFLOW was obtained from NASA-Ames personnel and was applied to the underside of the same waverider forebody. A solution for the forebody flowfield was obtained in about 45 minutes of Cray C-90 CPU time. A comparison of some of the salient features of the flowfields from the two solutions is discussed here.

Figure 12 shows a comparison of the Mach number contours from the OVERFLOW code and the STUFF code on the symmetry plane of the aircraft for the ramp surfaces. As can be seen, excellent engineering agreement is obtained from these two 3D solutions. Figure 13 shows a Mach number contour comparison between the STUFF and OVERFLOW solutions in the plane containing the cowl lip. It is clear that nearly identical flowfields are calculated, with some slight variation in the details at the corner. Figure 14 reveals that the slight variation at the corner might be due to the different assumed surface geometry for the two solutions. For the STUFF solution, a beveled chine was used, whereas in the OVERFLOW solution, a sharp corner was assumed. On the symmetry plane, the solutions are quite similar. These comparisons indicate that in excess of an order-of-magnitude speed up in computational efficiency can be obtained on the same grid by using the ARC3D algorithm in OVERFLOW over the present version of TUFF. Of course, the space-marched code (STUFF) has a much finer resolution in the streamwise direction and is still much faster than OVERFLOW where it can be used.

Another effort in the present reporting period was to examine the internal flowfield downstream of the cowl lip for a proposed inlet mounted on the waverider. First attempts to solve for the internal flow using the OVERFLOW code in a 2D version indicated that the inlet would unstart in the absence of bleed. This is a well-known computational, as well

as experimentally verified, fact for this particular set of inlet contours. In the present study, the OVERFLOW code boundary condition routine was modified to include arbitrary boundary layer bleed where required on any of the internal flow solid surfaces. The 2D version of the combined STUFF/SCRAM2D analysis discussed previously under the present grant was compared with the 2D OVERFLOW solution obtained with the identical bleed imposed. The results of this comparison are shown in the Mach number contours of Figure 15, where excellent agreement is shown, even in the minimum throat area of the inlet. Computational times involved for this 2D solution were approximately one hour of CPU time for the STUFF/SCRAM2D (most of the time is SCRAM2D) versus 45 seconds for the OVERFLOW code. This represents nearly a two order-of-magnitude speed up between the SCRAM2D and OVERFLOW codes, with nearly identical results being obtained.

In another validation effort, the boundary layer pitot profiles on the ramps of the Mach 5 inlet model obtained from CFD and experiment were compared. The CFD codes are the 2D versions of UPS, STUFF and OVERFLOW, all run with the Baldwin-Lomax turbulence model. Their results are compared with experimental data in Figure 16. Excellent agreement is shown between the various codes and the experimental data.

IV. CONCLUSIONS

An investigation was carried out to examine the three-dimensional nature of the flowfield over the lower surface of a hypothetical Mach 5 waverider aircraft. Large, three-dimensional flow effects in the absence of a full sidewall were shown. In addition, a new code, OVERFLOW, was applied to the waverider forebody and shown to produce virtually identical engineering results with an order of magnitude decrease in CPU time over previously-used codes. For the Mach 5 inlet contours the OVERFLOW results (with bleed added) were shown to be in excellent agreement with those from the SCRAM2D code, with nearly two order-of-magnitude decrease in computer time for the OVERFLOW code. Future efforts will concentrate on applying the both 3D and 2D versions of the OVERFLOW code to the internal flow portion of the waverider inlet, including the proposed subsonic diffuser.

Lewis/Langley Waverider

FIGURE 1 Lewis/Langley waverider configuration under study.

Mach Contours and Particle Traces Near Surface on Inlet Ramps

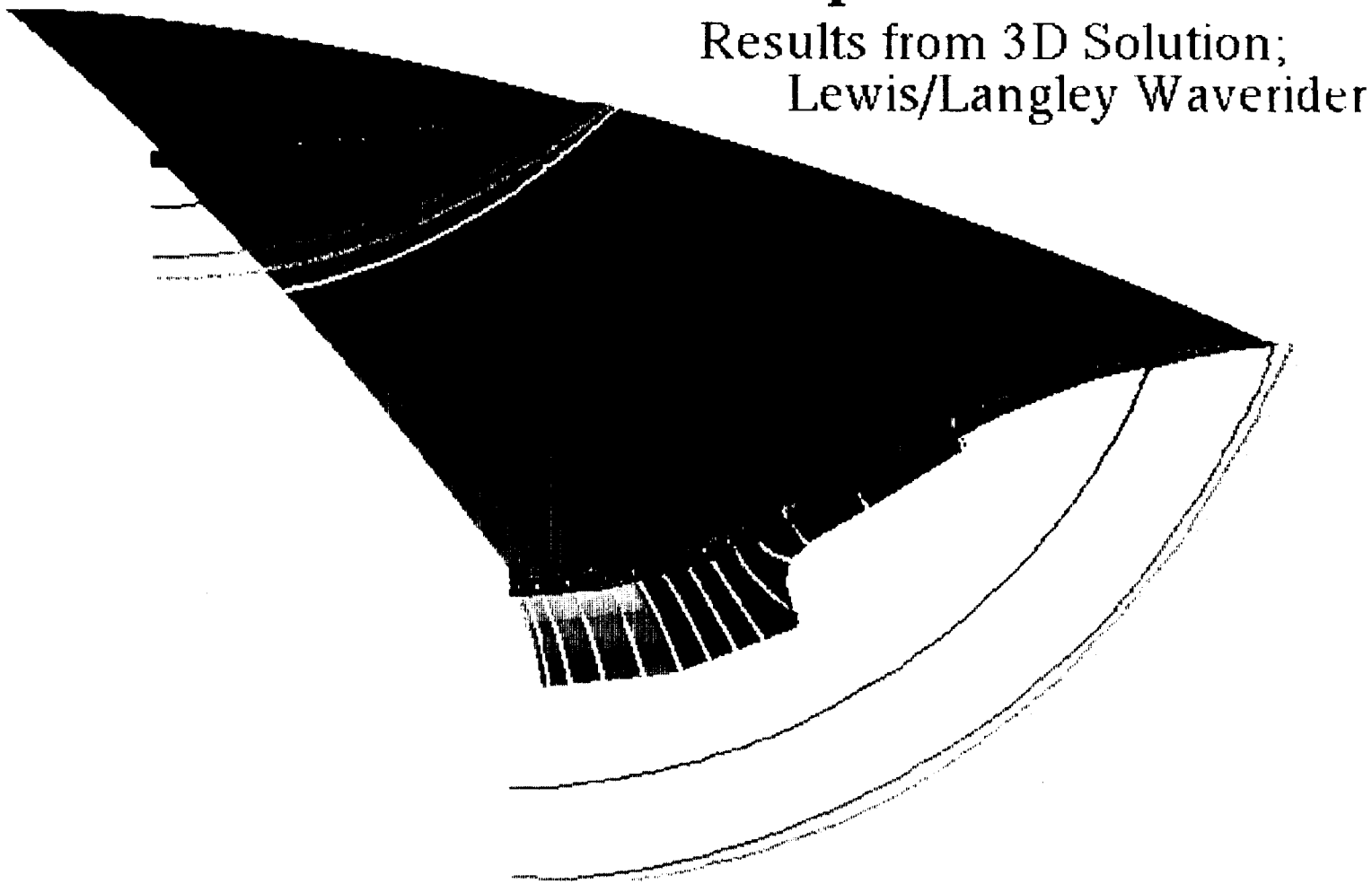

FIGURE 2 **Mach contours in two crossflow planes and particle traces near the inlet ramp surface; M = 5, α = 0.**

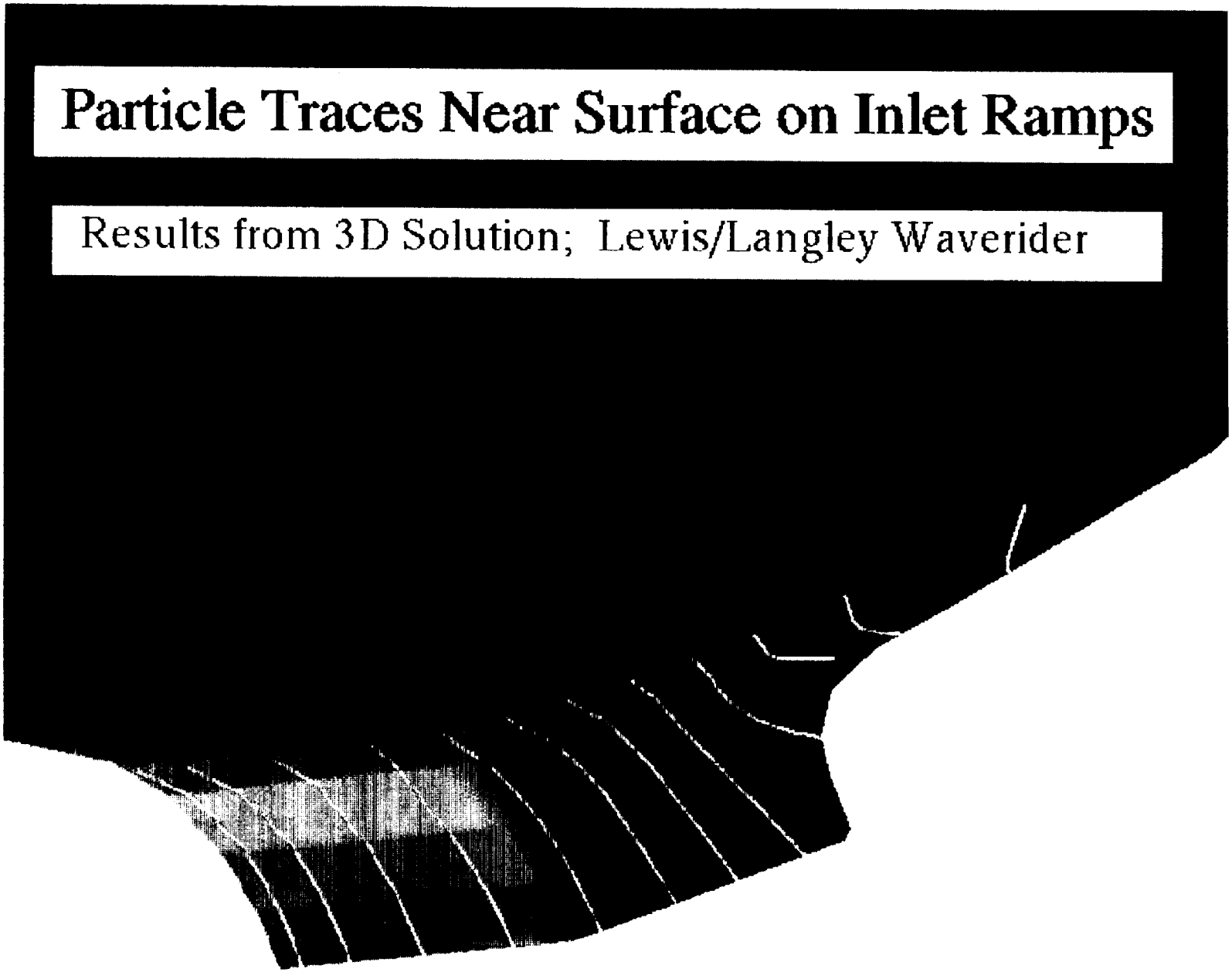

FIGURE 3 Particle traces near the surface of the inlet ramps; M = 5, α = 0.

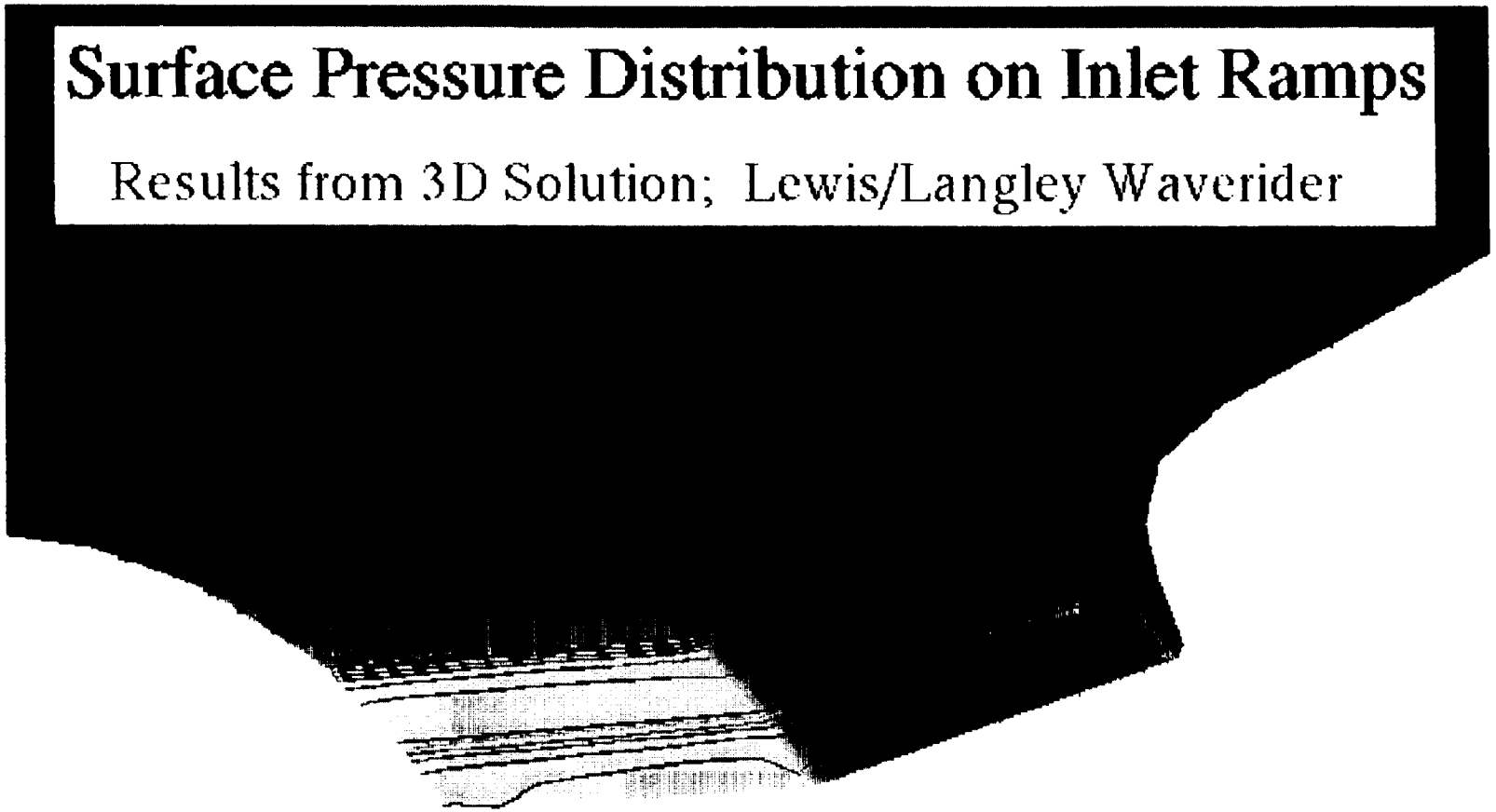

FIGURE 4 Surface pressure distribution on inlet ramps; M = 5, α = 0.

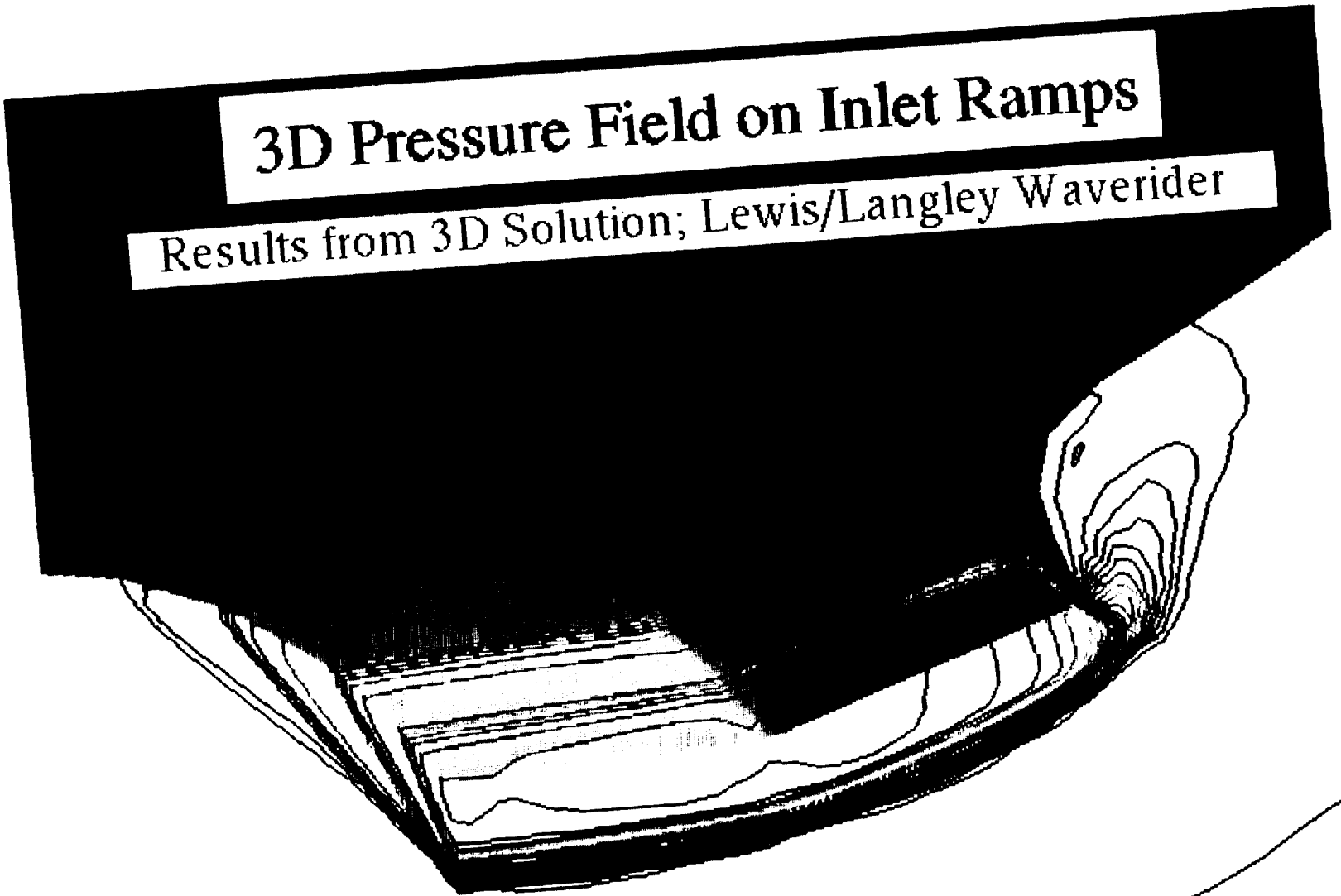

FIGURE 5 Pressure contours obtained on the symmetry plane of the aircraft, on the surfaces of the inlet ramps and in the cross flow plane containing the cowl lip; $M = 5, \alpha = 0$.

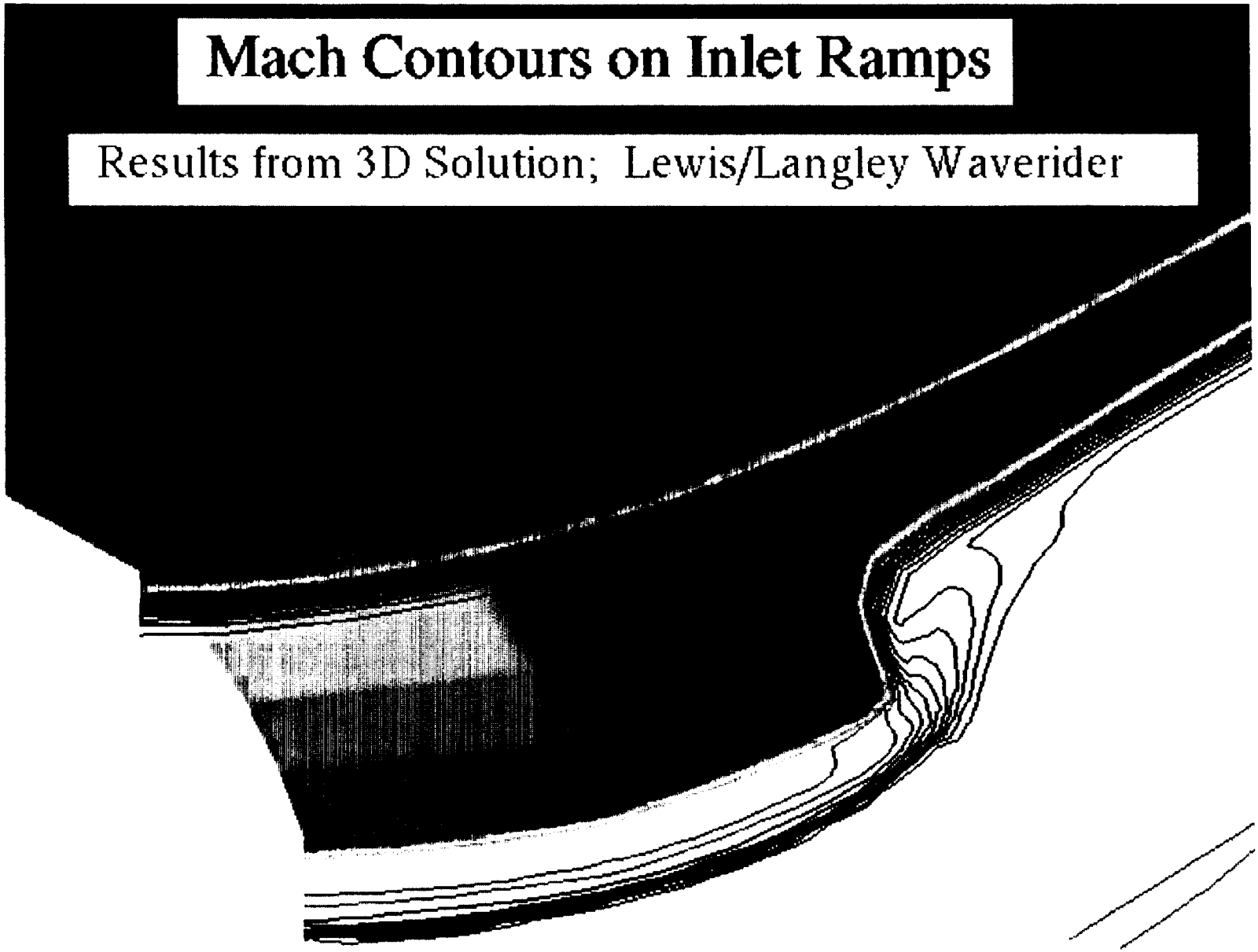

FIGURE 6 **Mach number contours in cross flow planes at the beginning of the ramps containing the cowl lip; M = 5, α = 0.**

Mach Contours on Inlet Ramps

Results from 3D Solution; Lewis/Langley Waverider

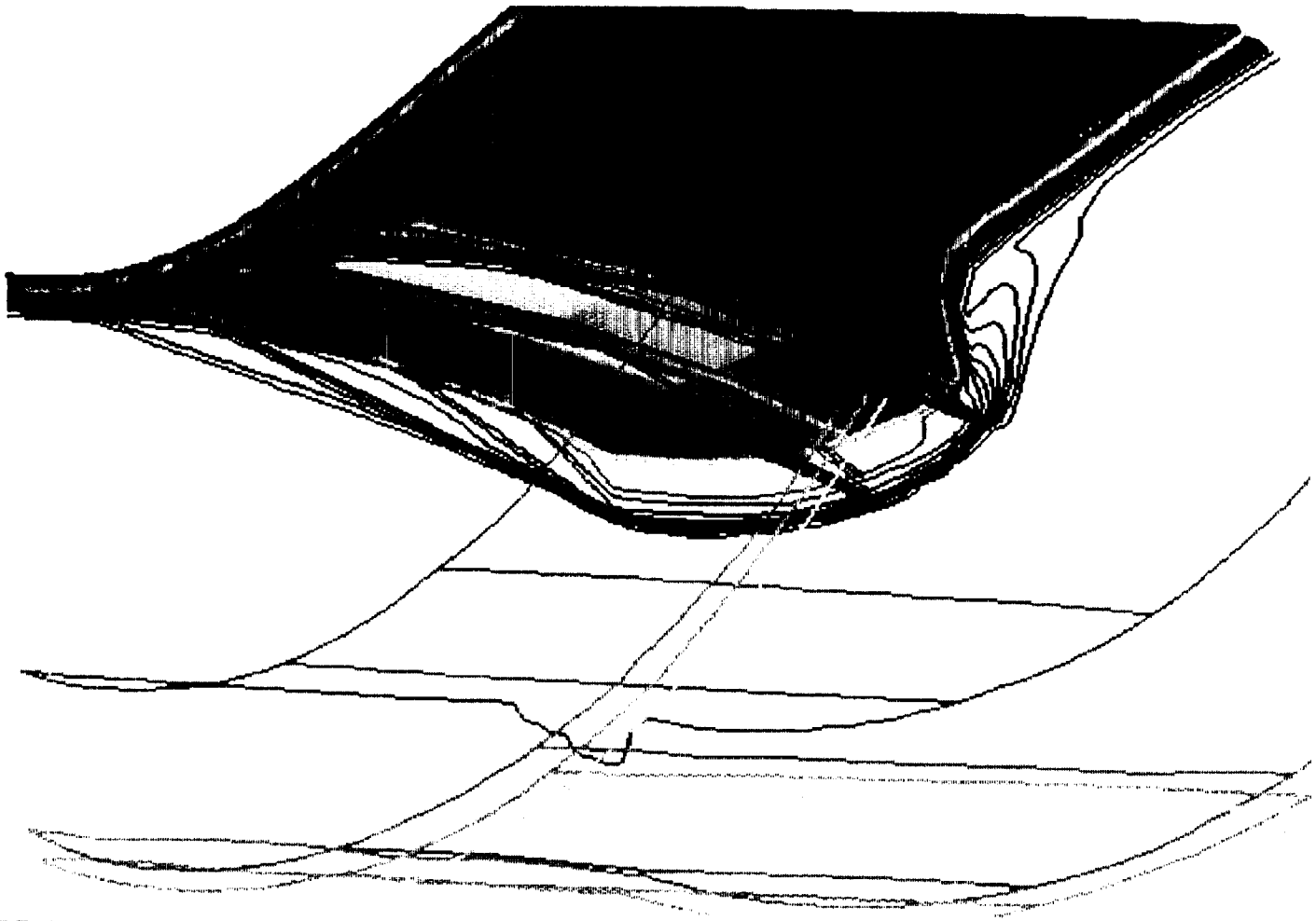

FIGURE 7 Mach number contours on the inlet ramps at three spanwise locations.

Mach Contours with Rake Positions

Results from 3D Solution; Lewis/Langley Waverider

Centerplane View

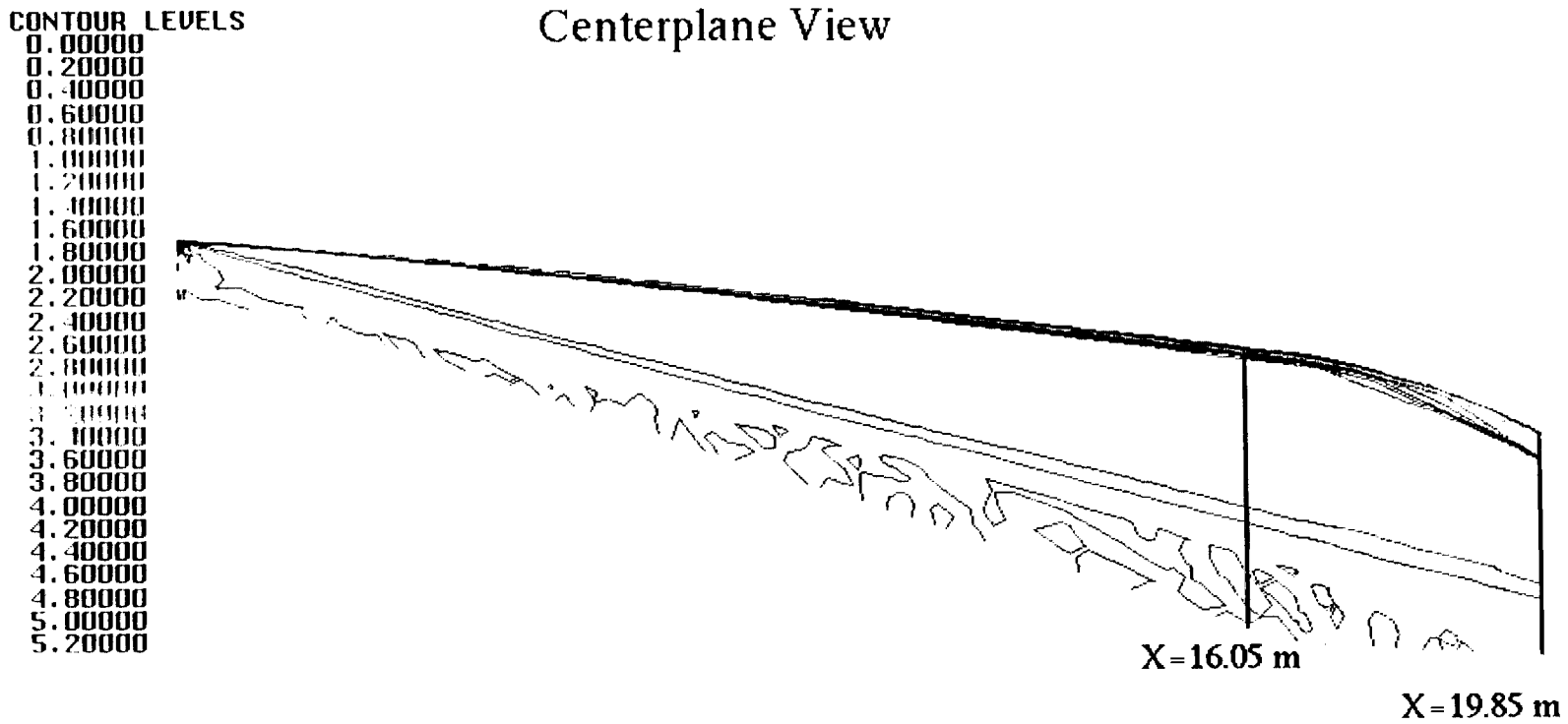

FIGURE 8 **Mach number contours and location of two computational rake planes (just ahead of 4.1 degree ramp and the cowl lip plane).**

Mach Contours with Rake Positions

Taken at X=16.05 m Just Ahead of 4.1 Degree Ramp

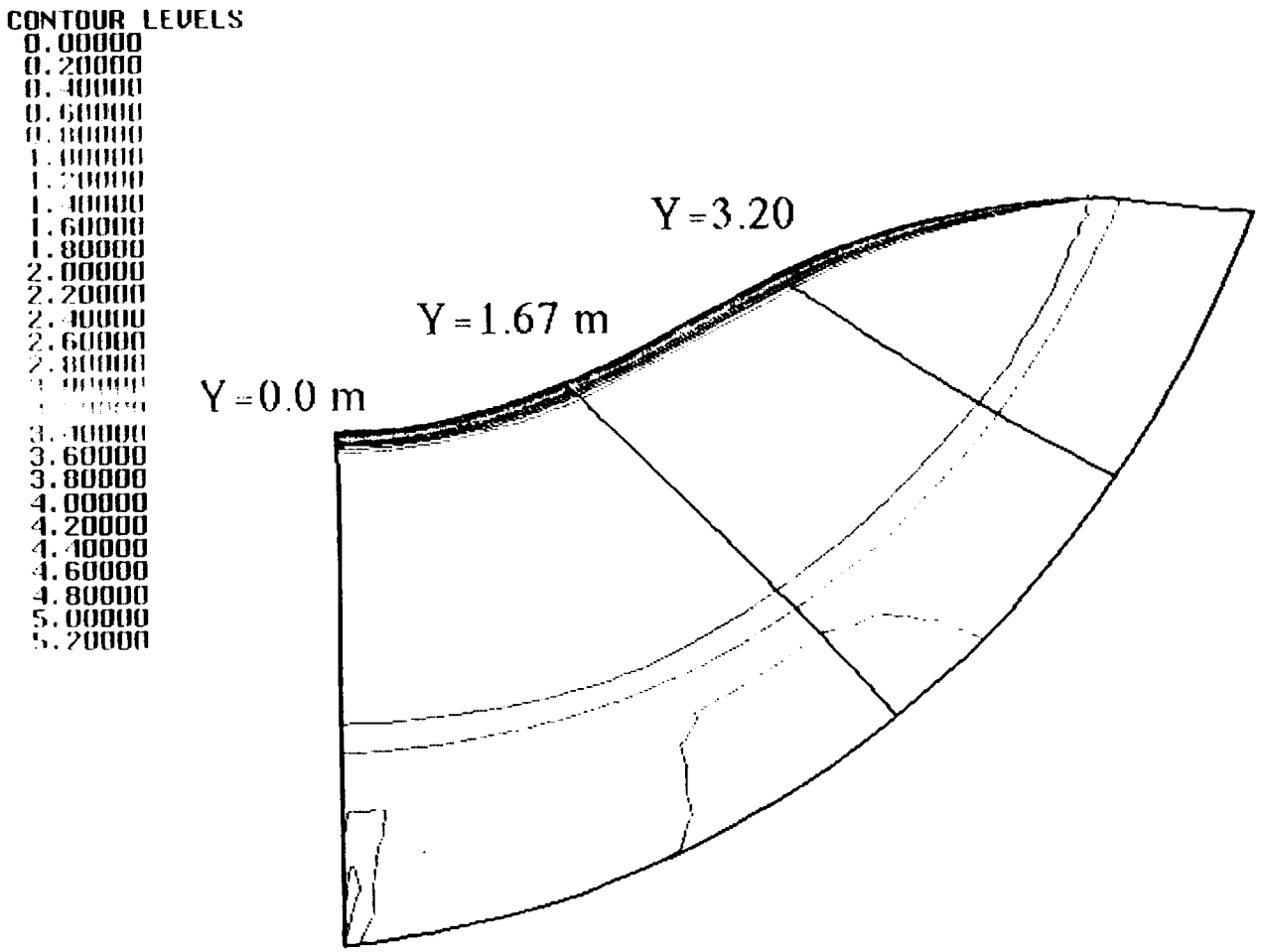

FIGURE 9 **Mach number contours and computational rake positions.**

a) Just ahead of 4.1 degree ramp

Mach Contours with Rake Positions

Taken at X=19.85 m (2.42 m from First Ramp)

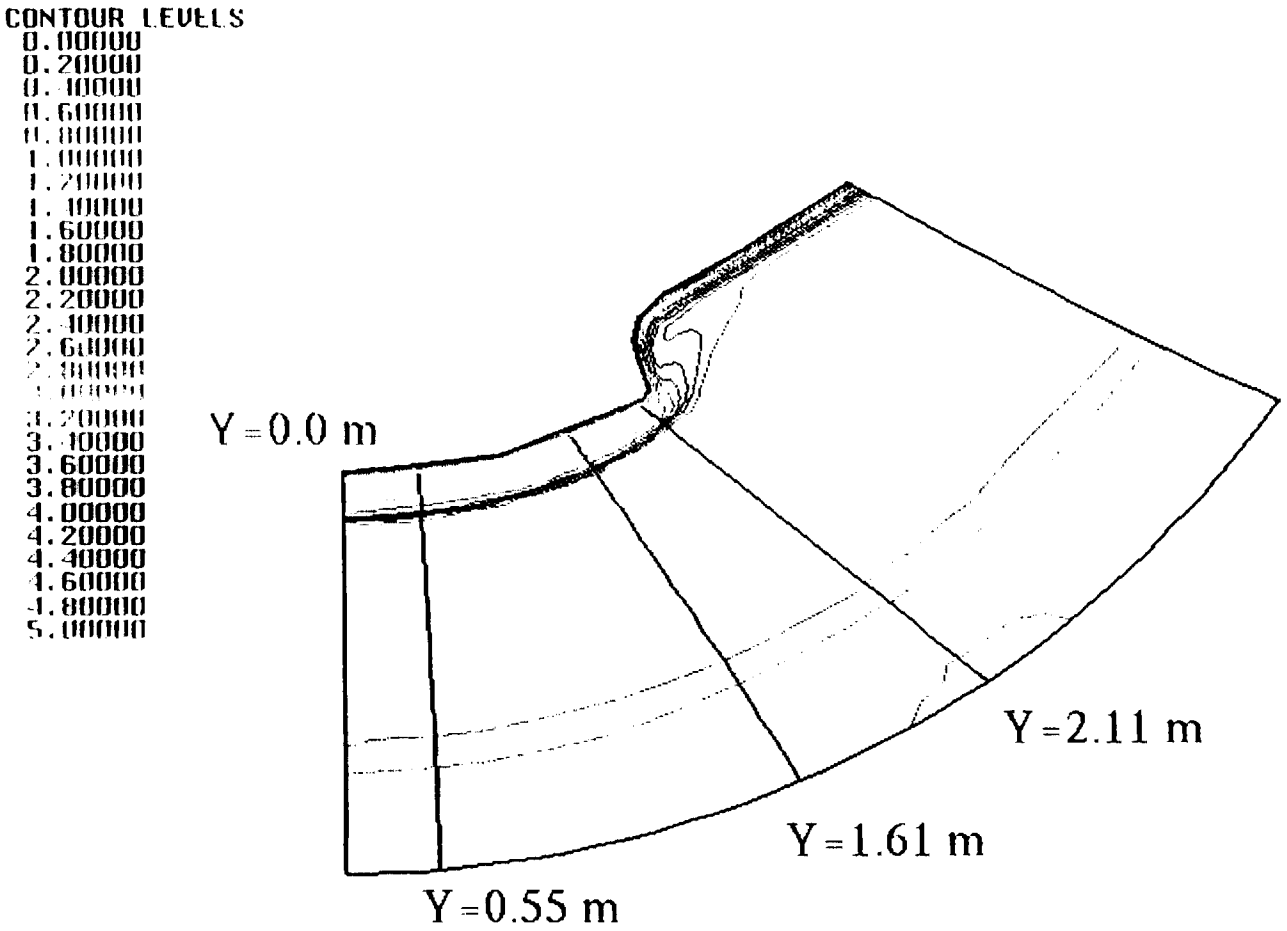

FIGURE 9 Concluded.

b) Cowl lip plane

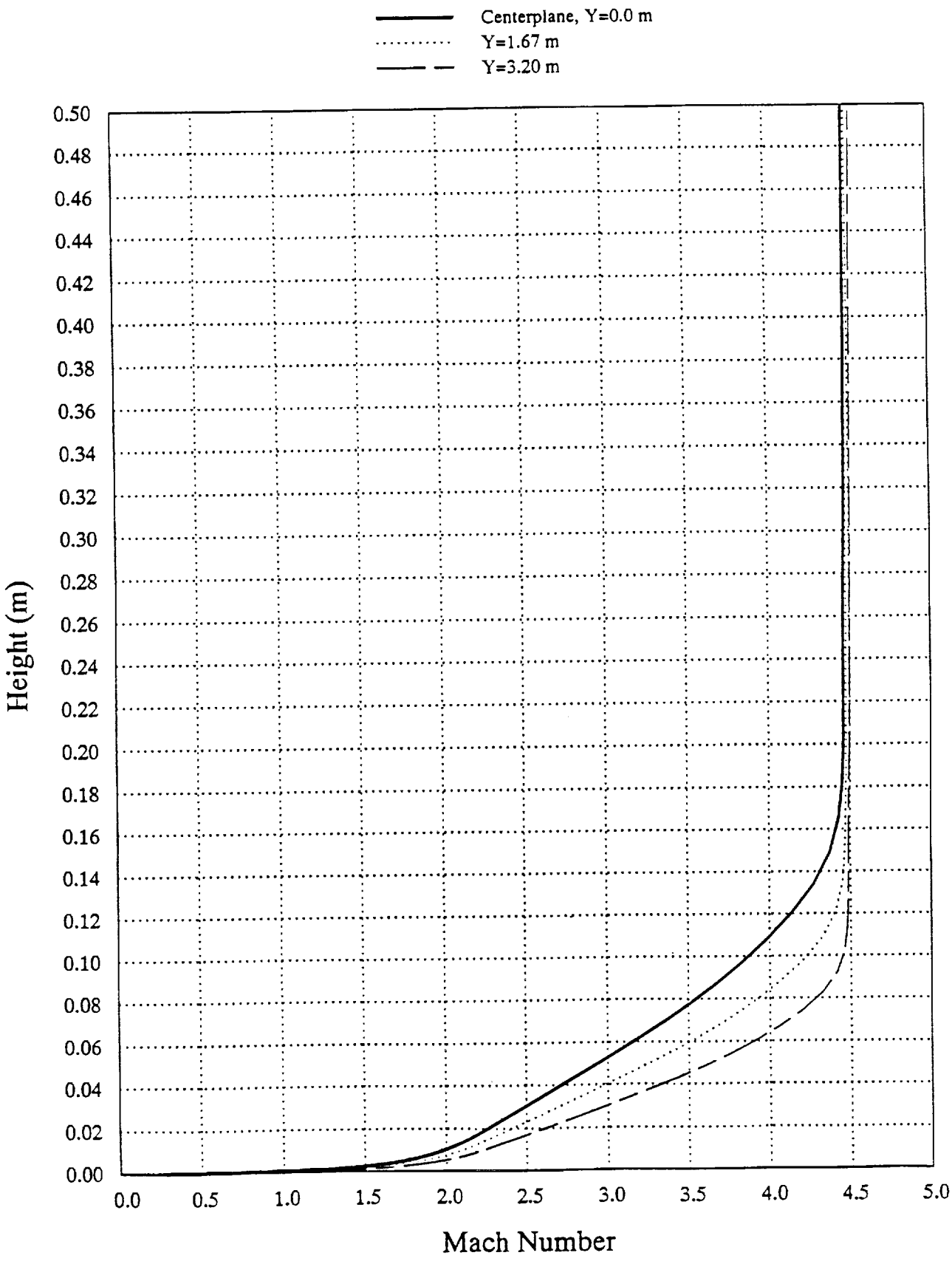

FIGURE 10 Mach number profiles at three spanwise locations just ahead of the 4.1 degree ramp.

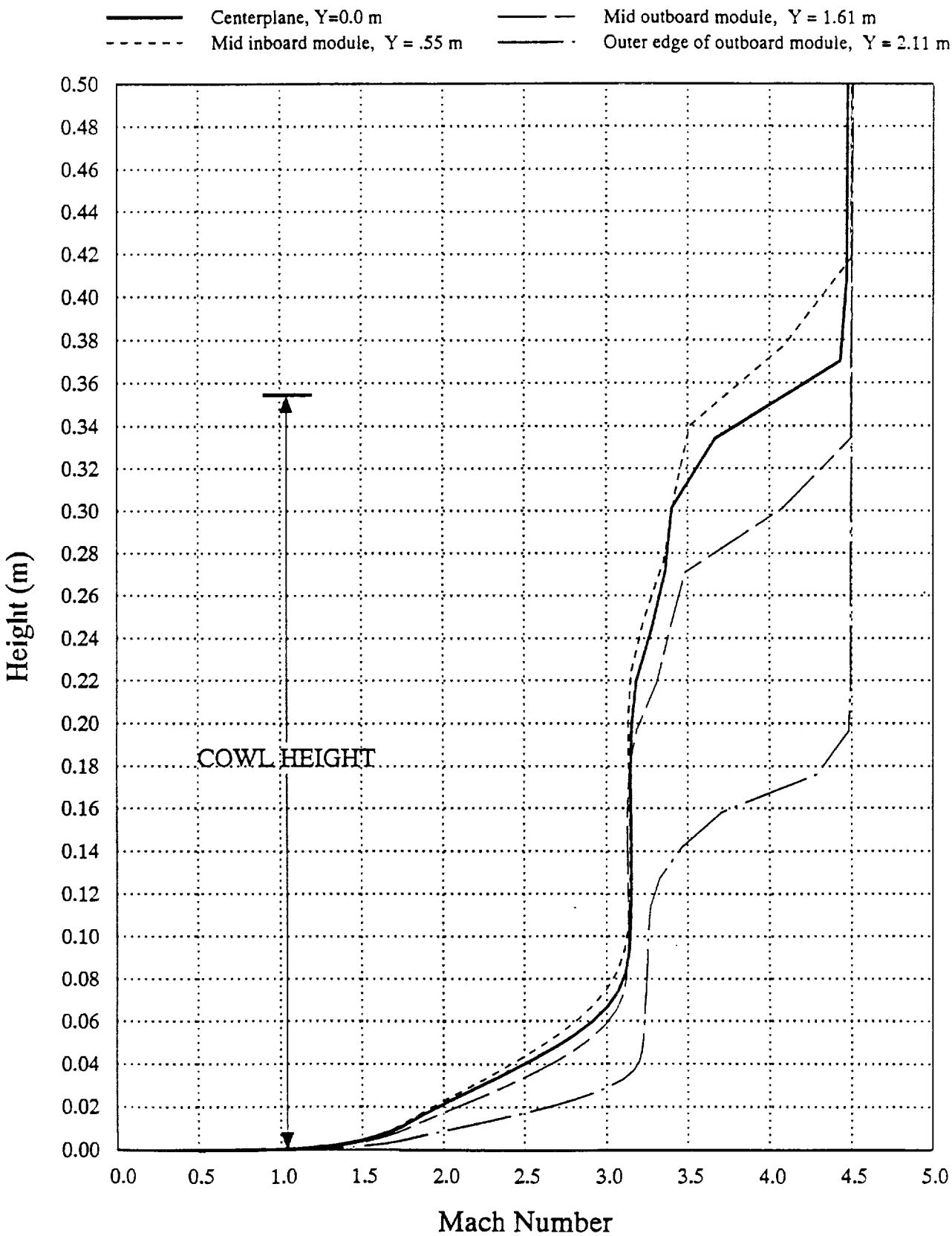

FIGURE 11 Mach number profiles at four spanwise locations in the cowl lip plane.

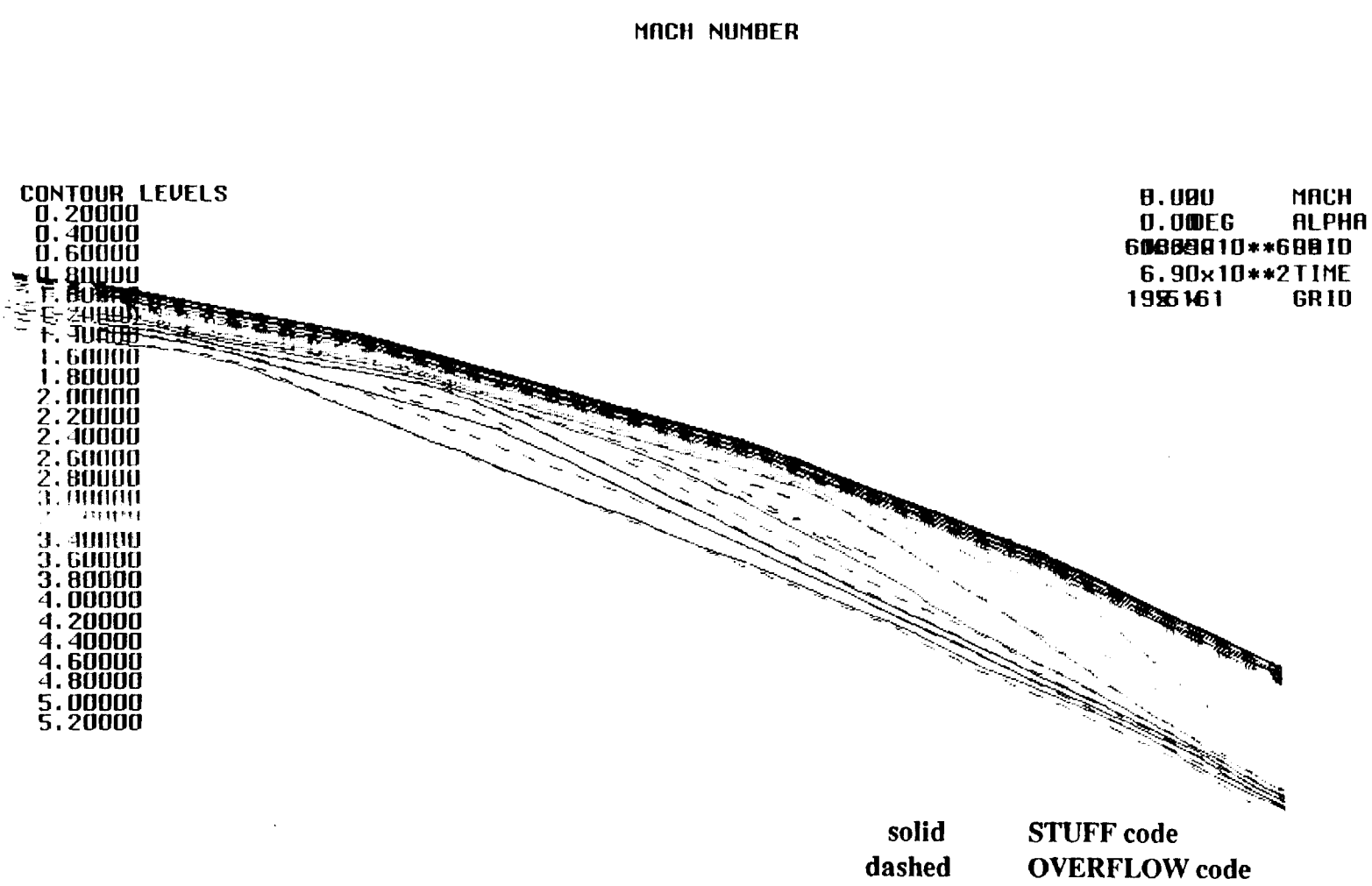

FIGURE 12 Comparison of Mach number contours from the 3D STUFF and OVERFLOW codes on the symmetry plane of the vehicle.

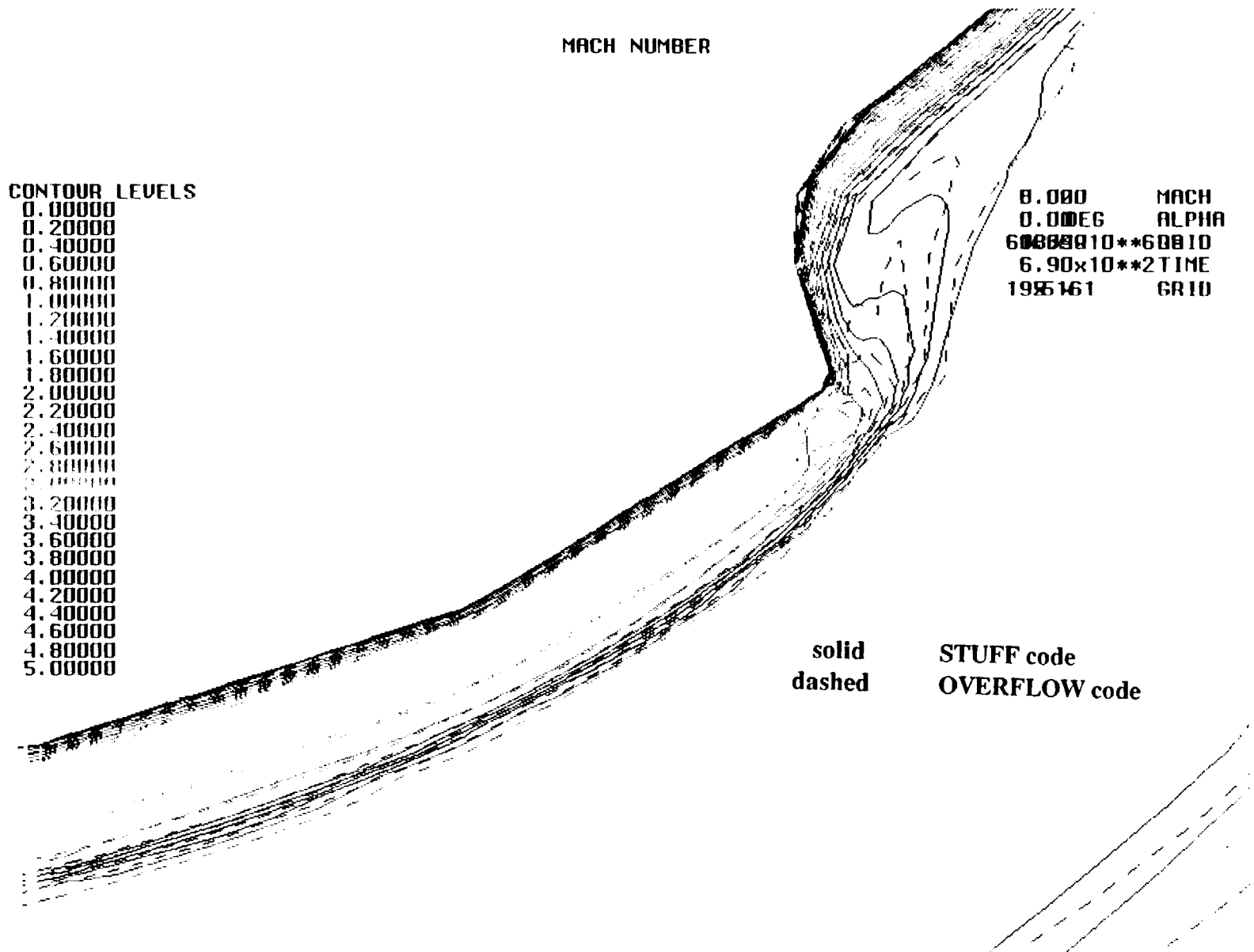

FIGURE 13 Comparison of Mach contours from the 3D STUFF and OVERFLOW codes in a crossflow plane containing the cowl lip.

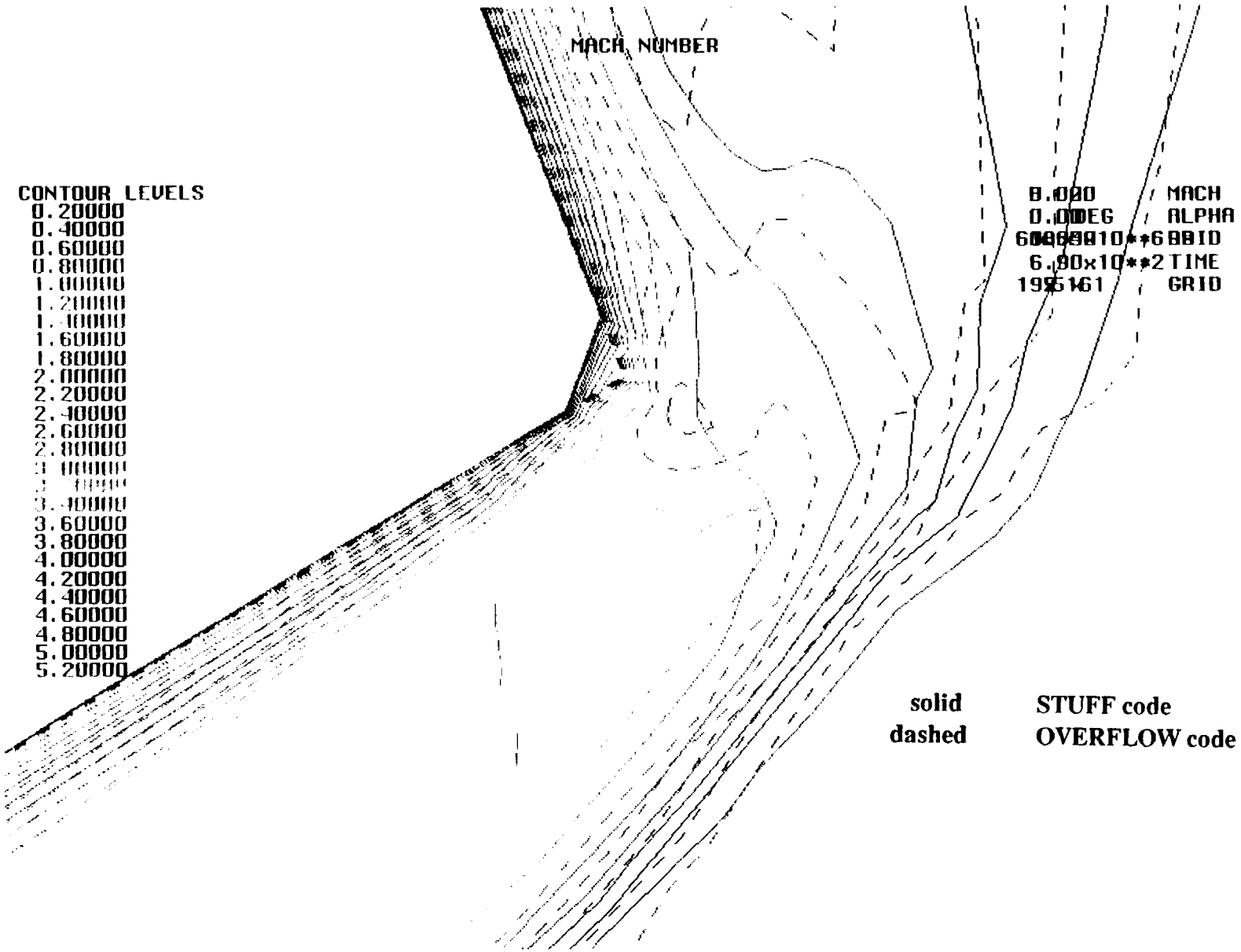

FIGURE 14 Detailed comparison of the STUFF and OVERFLOW Mach number contours near the corner flow region.

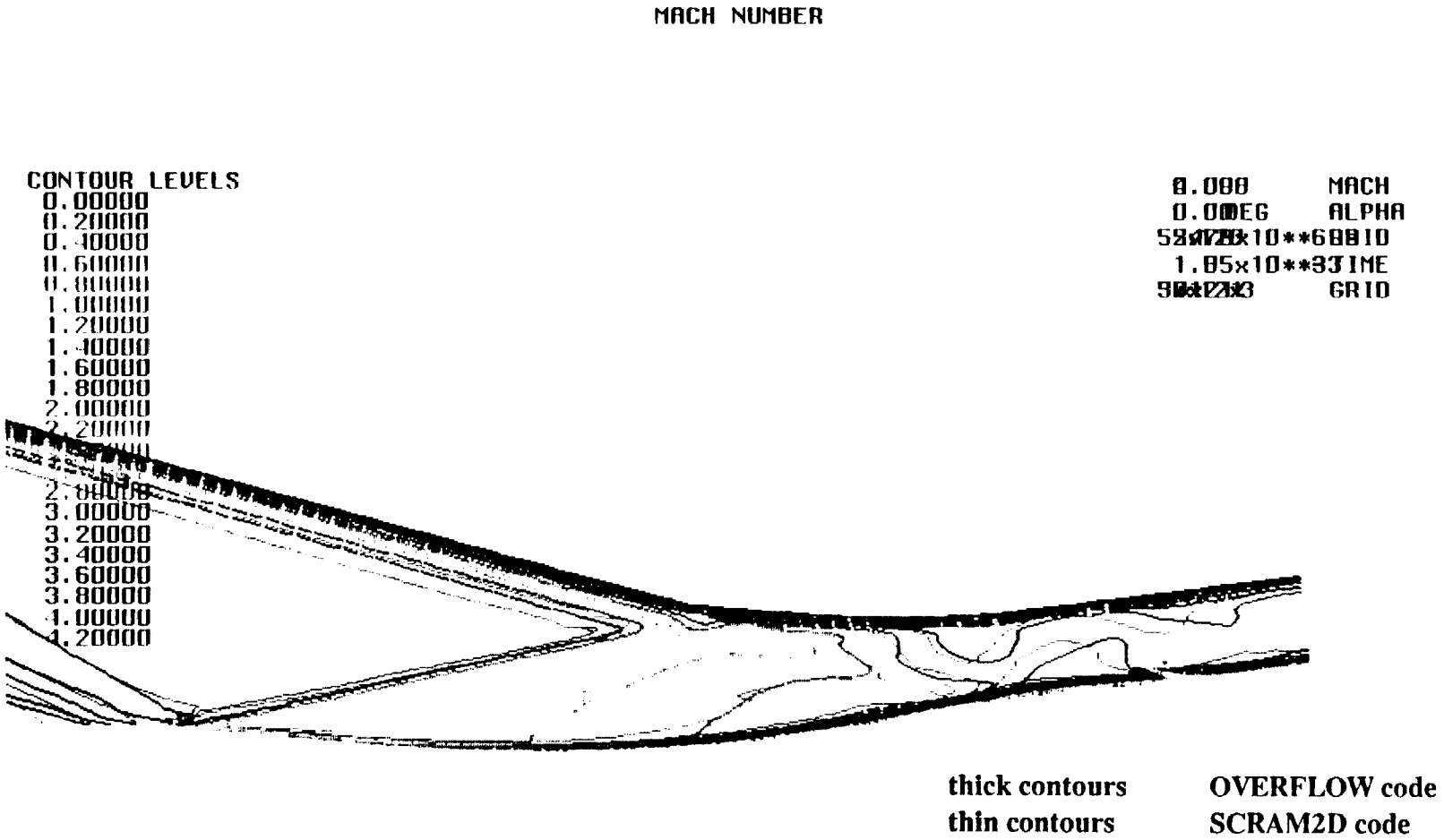

FIGURE 15 Comparison of Mach number contours for the internal flow solution from the hybrid STUFF/SCRAM2D and OVERFLOW (2D version) for the Mach 5 inlet model.

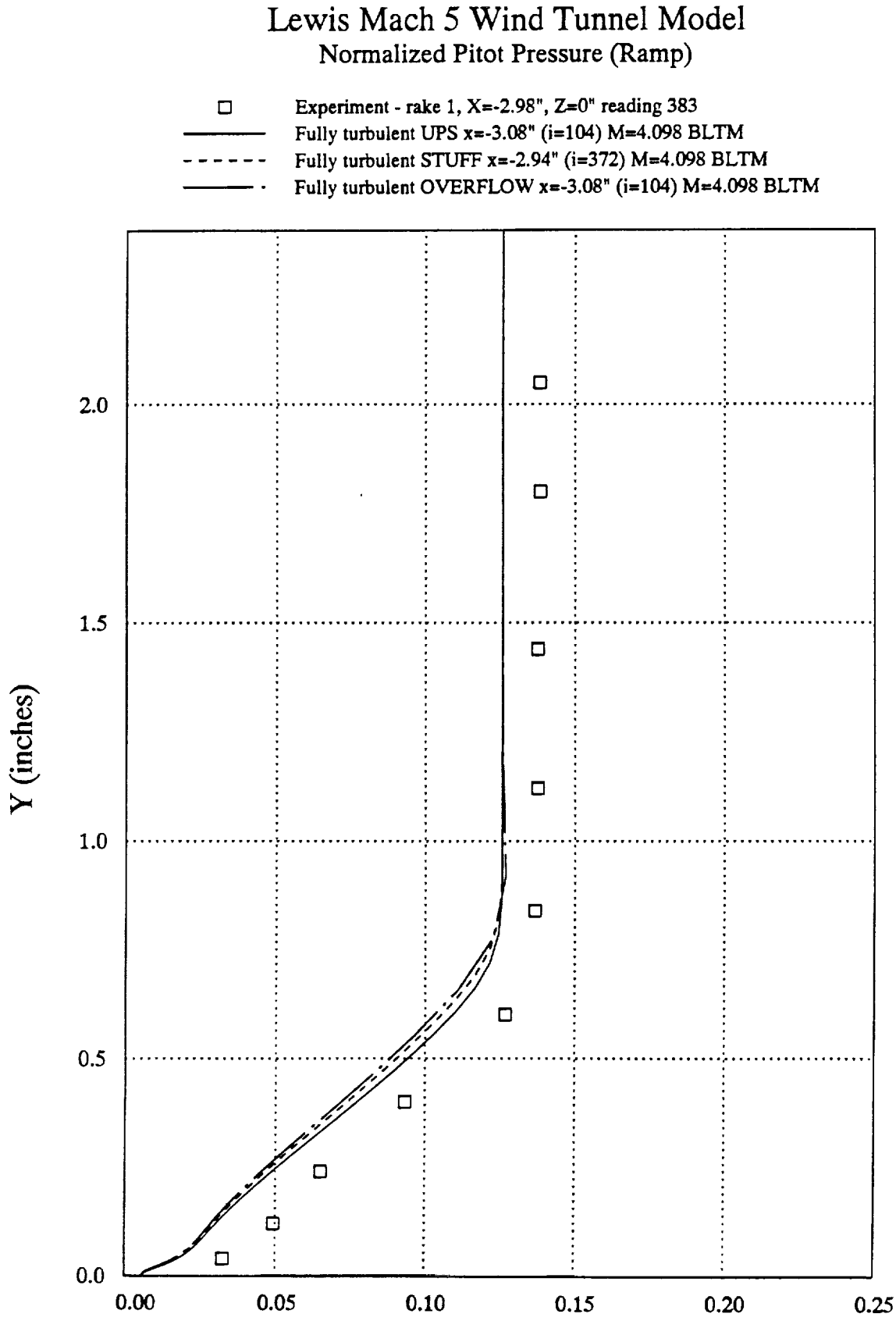

FIGURE 16 **Comparison of calculated and experimental pitot pressure profile for the Mach 5 inlet model ramps system from UPS and STUFF codes and the new OVERFLOW code.**

a) Rake 1; x = -3.0".

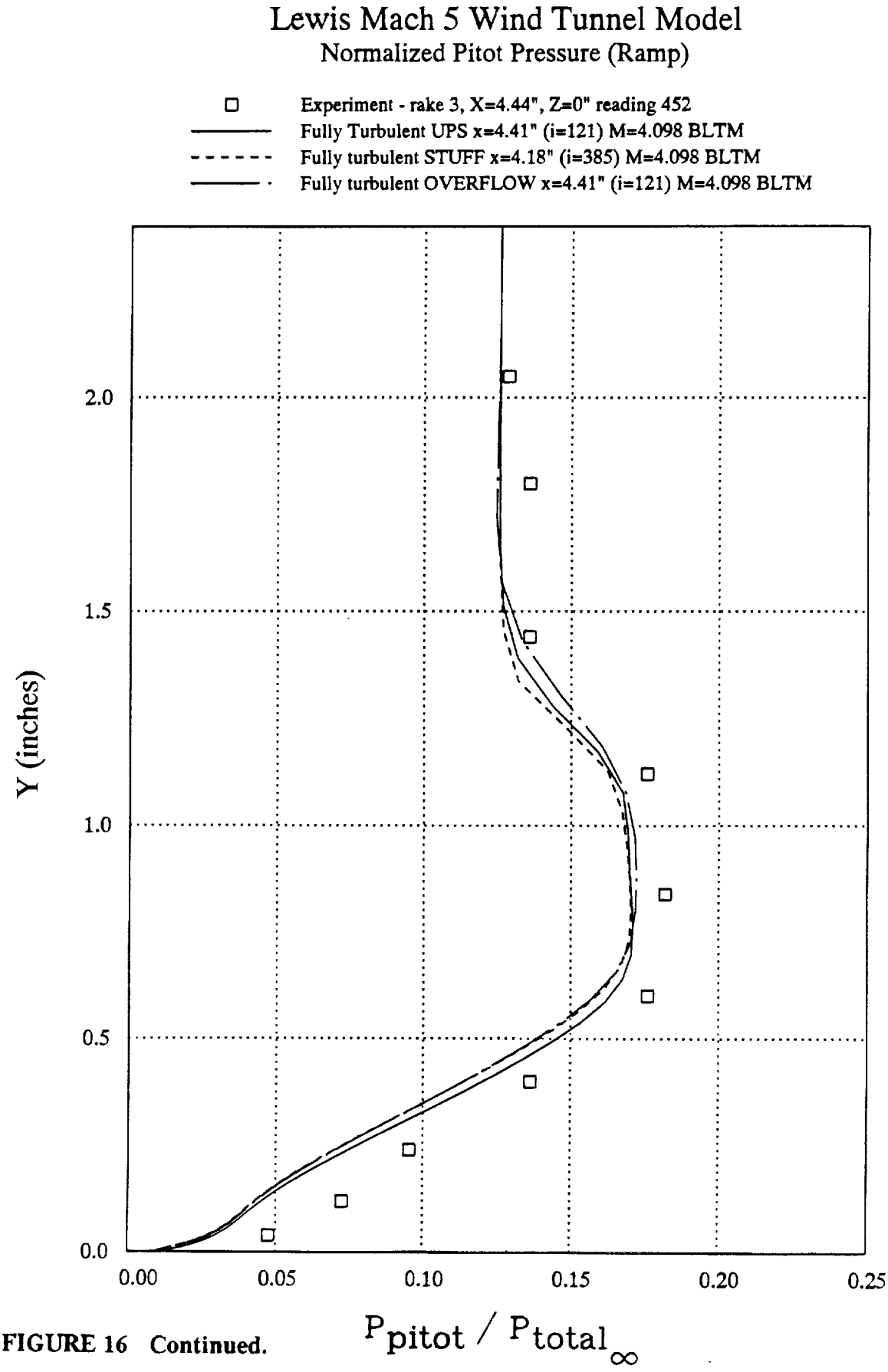

FIGURE 16 Continued.

b) **Rake 3; x = 4.4".**

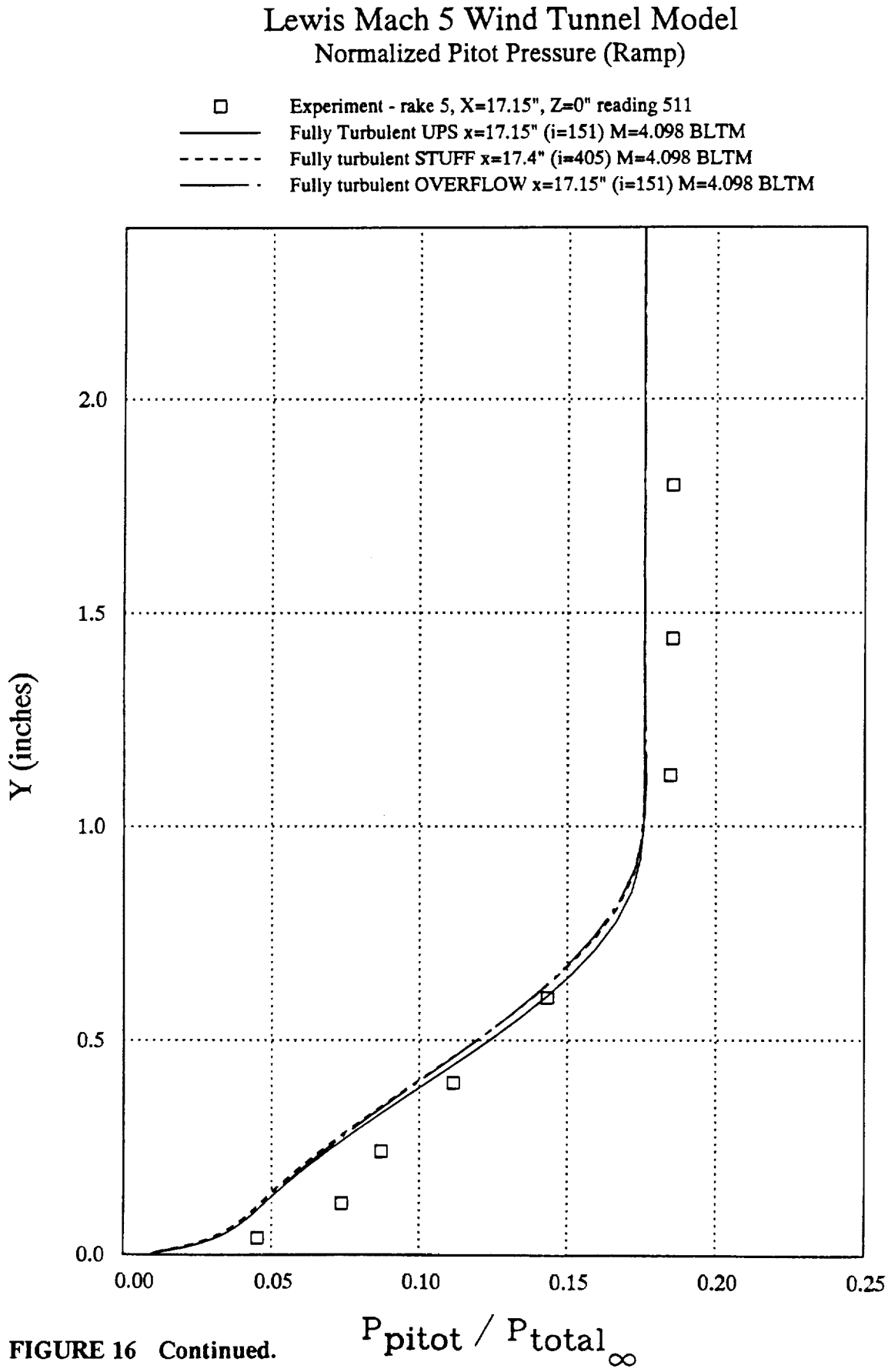

FIGURE 16 Continued.

c) **Rake 5, x = 17.2".**

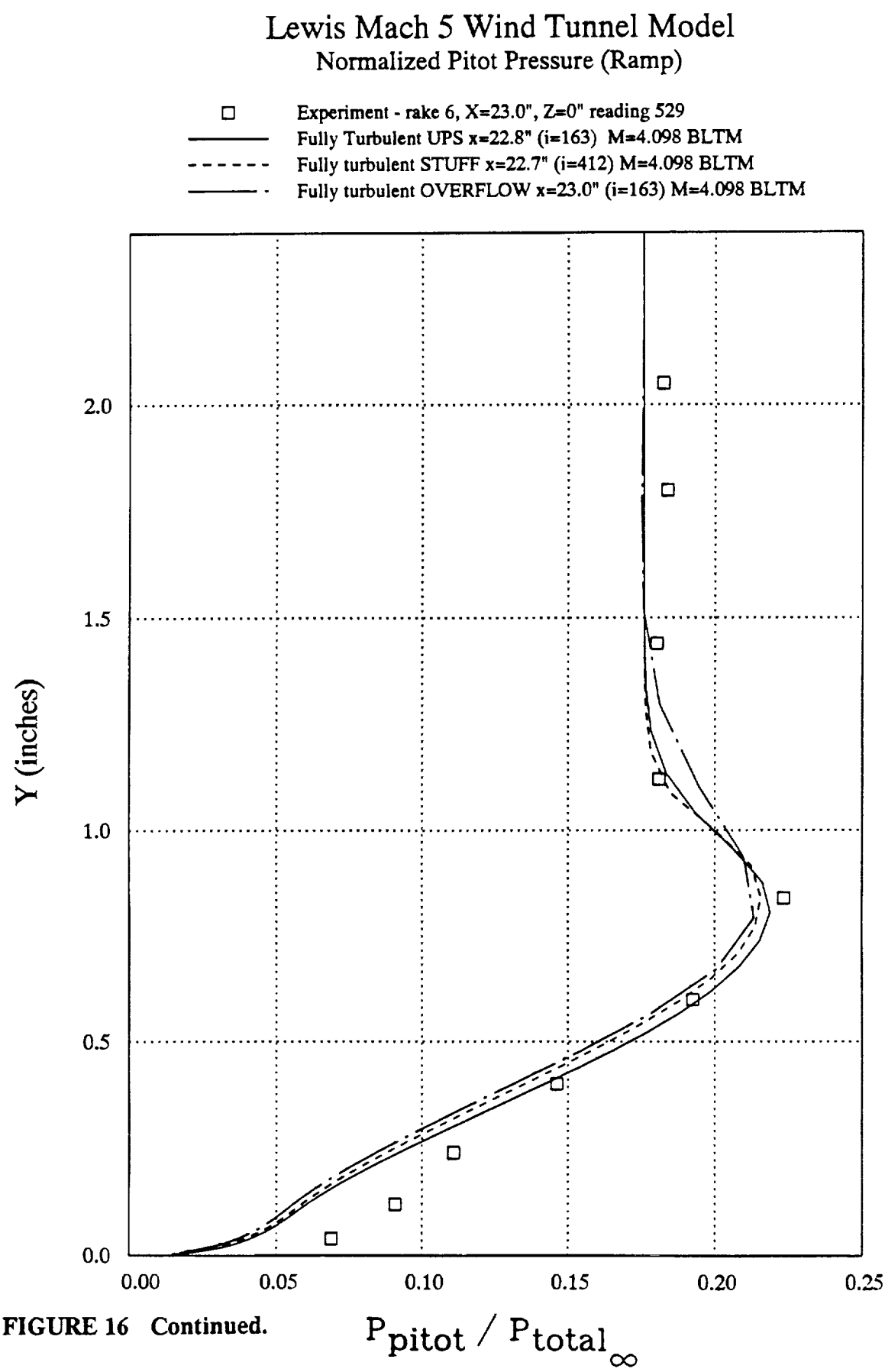

FIGURE 16 Continued.

d) **Rake 6; x = 22.8".**

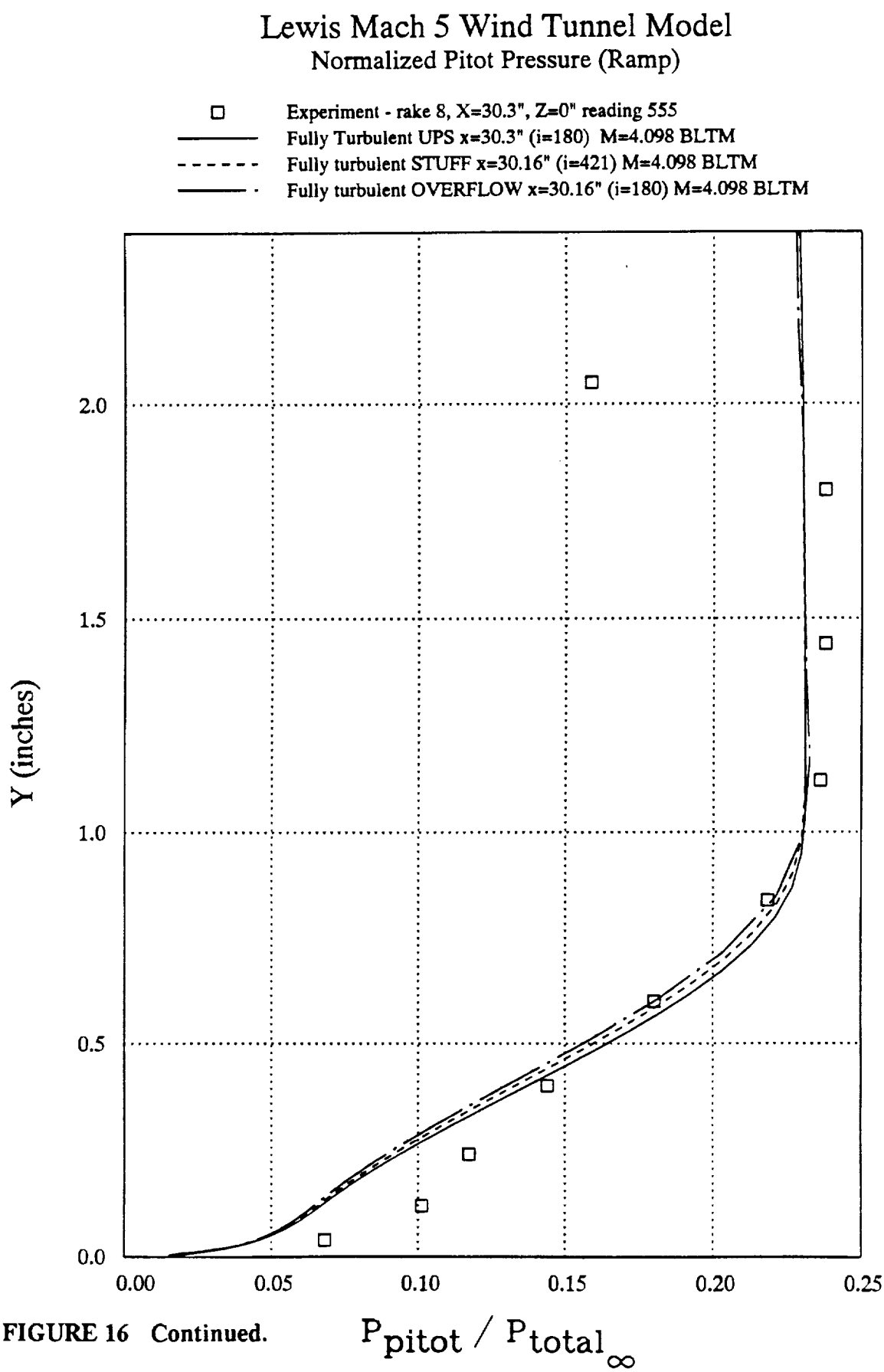

FIGURE 16 Continued.

e) **Rake 8; x = 30.2".**

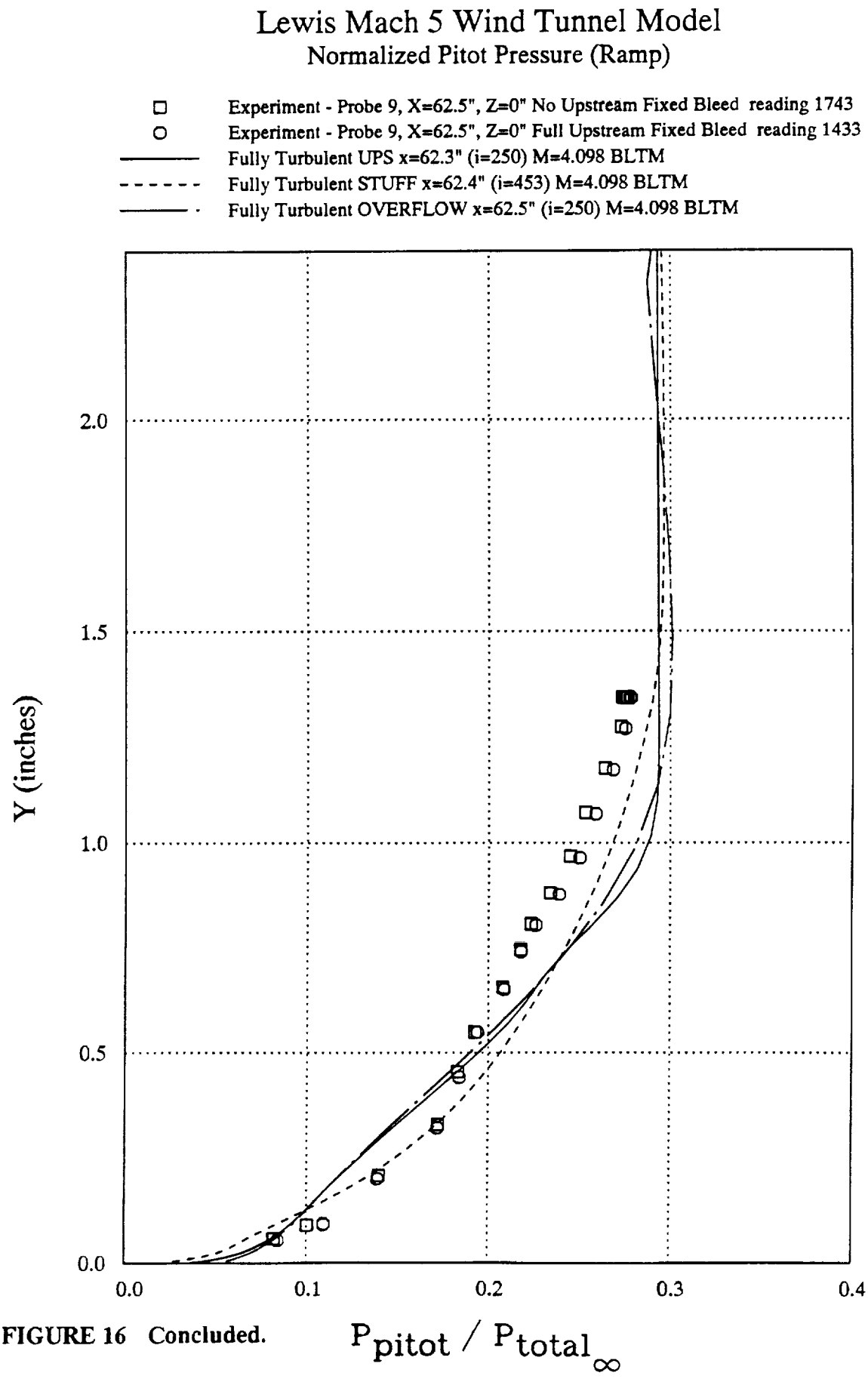

FIGURE 16 Concluded.

f) **Probe 9; x = 62.5".**